

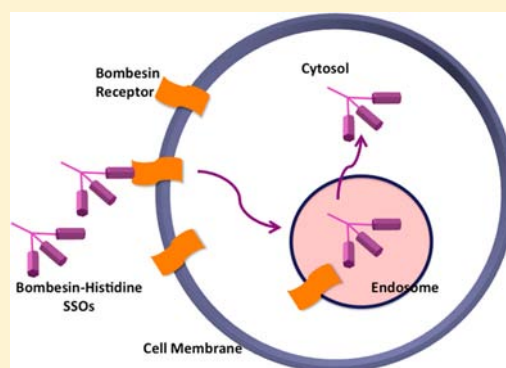
Conjugation with Receptor-Targeted Histidine-Rich Peptides Enhances the Pharmacological Effectiveness of Antisense Oligonucleotides

Osamu Nakagawa, Xin Ming, Kyle Carver, and Rudy Juliano*

Division of Molecular Pharmaceutics, UNC Eshelman School of Pharmacy, University of North Carolina, Chapel Hill North Carolina 27599, United States

S Supporting Information

ABSTRACT: Ineffective delivery to intracellular sites of action is one of the key limitations to the use of antisense and siRNA oligonucleotides as therapeutic agents. Here, we describe molecular scale antisense oligonucleotide conjugates that bind selectively to a cell surface receptor, are internalized, and then partially escape from nonproductive endosomal locations to reach their sites of action in the nucleus. Peptides that include bombesin sequences for receptor targeting and a run of histidine residues for endosomal disruption were covalently linked to a splice switching antisense oligonucleotide. The conjugates were tested for their ability to correct splicing and up-regulate expression of a luciferase reporter in prostate cancer cells that express the bombesin receptor. We found that trivalent conjugates that included both the targeting sequence and several histidine residues were substantially more effective than conjugates containing only the bombesin or histidine moieties. This demonstrates the potential of creating molecular scale oligonucleotide conjugates with both targeting and endosome escape capabilities.



INTRODUCTION

There are multiple approaches for employing oligonucleotides to influence the extent and pattern of gene expression. This includes using conventional antisense or siRNA molecules to selectively degrade mRNA,^{1,2} antagomirs to block the actions of miRNAs,³ splice switching oligonucleotides (SSOs) to alter gene expression patterns,⁴ decoys to block transcription factors,⁵ CpG rich oligonucleotides to stimulate the immune system,⁶ and triplex oligonucleotides for targeted mutagenesis.⁷ However, despite much research and the advent of multiple clinical trials,^{8,9} the development of oligonucleotides as pharmacological agents has been impeded by the fact that delivery of these large, highly polar molecules to their sites of action in the cytosol or nucleus is a very challenging problem.^{10,11}

There have been two broad approaches to the delivery of oligonucleotides. One has been to incorporate oligonucleotides into various nanocarriers including lipoplexes formed using cationic lipids^{12,13} and polyplexes made with cationic polymers^{14,15} or with cationic cell penetrating peptides.^{16,17} Another approach has been to create molecular-scale conjugates where oligonucleotides are covalently linked to ligands that can bind with high affinity to specific cell surface receptors and thus promote entry via endocytotic pathways. This includes aptamer–siRNA chimeras that interact with the PMSA receptor in prostate cancer cells,¹⁸ a conjugate of siRNA with a CpG oligonucleotide to promote uptake via Toll-like Receptor 9,¹⁹ our own previous work using SSOs or siRNAs

conjugated to peptide ligands for integrins^{20,21} or for G Protein Coupled Receptors (GPCRs),²² as well as other studies using peptide²³ or carbohydrate ligands.²⁴

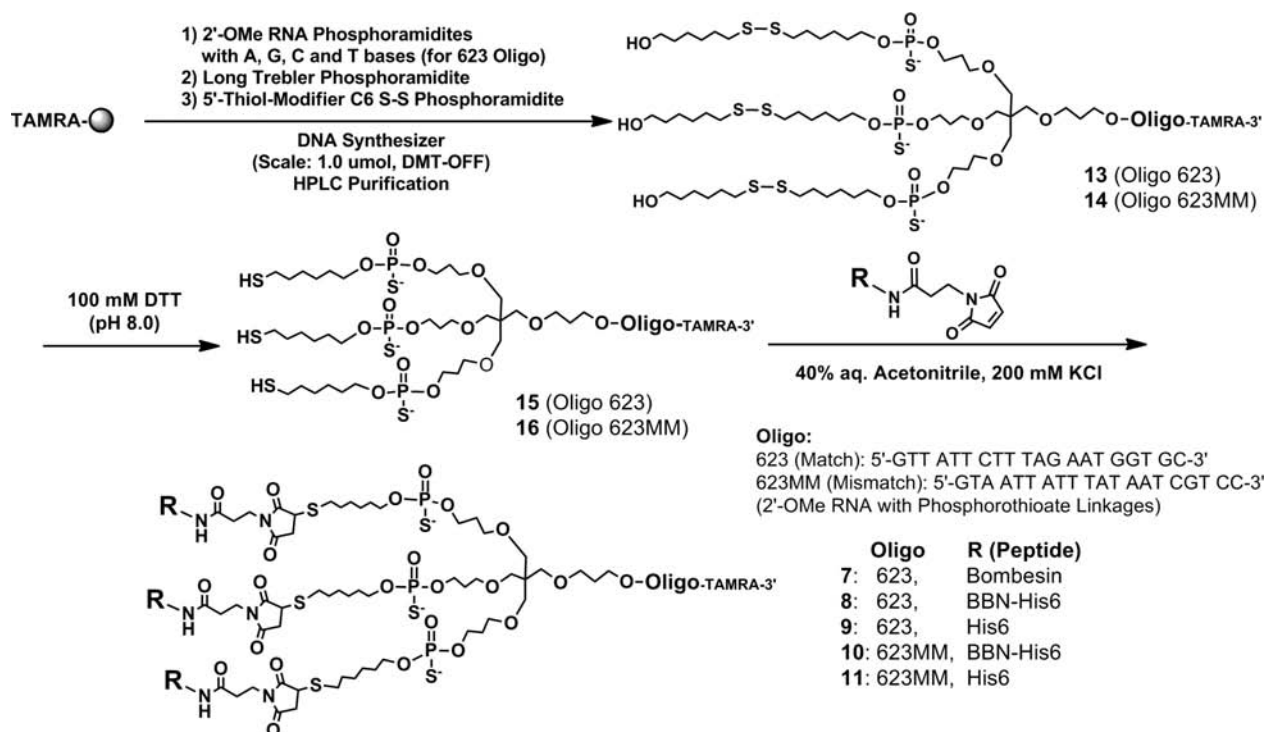
A major difference between the two approaches is the utilization of membrane-disrupting strategies. Thus, cationic lipoplexes can enhance oligonucleotide delivery to the cytosol and nucleus by creating transient nonbilayer perturbations of cellular membranes.²⁵ Some cationic polymers can cause endosome destabilization through the ‘proton sponge effect’.²⁶ By contrast, none of the receptor-targeted oligonucleotide conjugates discussed above had membrane-disrupting functions intentionally incorporated in their design. In the current study, we sought to evaluate the merits of including both a targeting ligand and an endosome-destabilizing moiety into molecular scale oligonucleotide conjugates. For targeting we chose a bombesin-like peptide sequence (BBN) that binds with high affinity to BB2, a GPCR that is highly expressed in various carcinoma cells.²² For endomembrane disruption we chose to use multiple histidine moieties that are titratable at the pH range found in endosomes. There has been previous work using histidine-rich peptides to promote the delivery of plasmid DNA and of oligonucleotides.^{26,27} However, this has largely been via the formation of nanoparticle complexes between the peptides and the nucleic acid. Here we demonstrate that the inclusion of

Received: October 28, 2013

Revised: December 13, 2013

Published: December 15, 2013

Scheme 1



histidine residues into a multivalent receptor-targeted conjugate can substantially enhance functional delivery and biological effects of the oligonucleotide.

EXPERIMENTAL PROCEDURES

Reagents and Materials. All oligonucleotide (ON) synthesis reagents were purchased from Glen Research (Sterling, VA). All maleimide-terminated peptides were purchased as custom order products from AnaSpec (Fremont, CA) or Bachem (Torrance, CA). The peptides were characterized by HPLC and mass spectrometry by the manufacturer. The peptides used in the conjugation reactions are depicted in Table S1 of the Supporting Information.

Numbering of Compounds. The oligonucleotides and conjugates associated with the bolded numerals below are shown in Scheme 1 and in Table S2 of the Supporting Information.

Synthesis of Monovalent Bombesin-His6 Conjugated 623 Oligonucleotide (BBN-His6-623-T, 3). The 623 oligonucleotide with a 3' TAMRA fluorophore but without any 5' conjugation (1, 623-T) as well as the monomeric bombesin conjugate (2, BBN-623-T) have been previously described.²² To prepare 3 a previously described²⁰ thiol oligonucleotide (12 (42.5 nmol) was reacted with maleimide-containing bombesin-His6 peptide (118.8 nmol) in a reaction buffer (final salt concentration adjusted to 400 mM KCl, 40% aqueous CH_3CN , total solution 400 μL). The reaction mixture was vortexed and allowed to stand for 3 h. The conjugate was dialyzed versus milli-Q water (with a Thermo SCIENTIFIC, Slide-A-Lyzer Dialysis Cassette, 3500 MWCO). The structure of the conjugate was determined by MALDI-TOF mass spectrometry (AB SCIEX Voyager DE-PRO). The other monovalent conjugates (4, 5, 6) were also synthesized using the same procedure.

Synthesis of TAMRA-623-TRI-C₆-S-S-C₆-OH (13). The branched oligonucleotide 13 was synthesized with an Applied Biosystems 3400 DNA synthesizer using DMT-OFF mode. 3'-TAMRA CPG (1000 Å, 1 μmol scale) was used. Tris-2,2,2-[3-(4,4'-dimethoxytrityloxy)propyloxymethyl]-methyleneoxypropyl-[(2-cyanoethyl)-(N,N-diisopropyl)]-phosphoramidite (termed Long trebler phosphoramidite) was used to prepare a three-branched ON. Thereafter, 1-O-dimethoxytrityl-hexyl-disulfide, 1'-[(2-cyanoethyl)-(N,N-diisopropyl)]-phosphoramidite (termed 5'-thiolmodifier C6 S-S phosphoramidite) was used to introduce a thiol linker to the 5'-terminal. The coupling times for the phosphoramidites of 2'-O-Me RNA, long trebler linker, and modifier C6 S-S linker were 300, 900, and 900 s, respectively. 5-(Ethylthio)-1H-tetrazole was used as an activator (0.25 M solution in acetonitrile), 5% phenoxyacetic anhydride in tetrahydrofuran/pyridine as a CAP mix A, and Beaucage reagent was used to introduce the internucleotide phosphorothioate backbone. Prior to deprotection, the CPG support was treated with a 10% solution of diethylamine in acetonitrile. ON was simultaneously cleaved from the CPG support and deprotected using a mixture of *tert*-butylamine:methanol:water (1:1:2) at 50 °C for 16 h. Purification of the oligonucleotide was carried out by reverse-phase HPLC using a ZORBAX 300 SB-C18 column (9.4 mm \times 250 mm). Finally, the sample was desalted by gel filtration with a GE Healthcare illustra NAP-25 column. The structure of the ON (13) was determined by ESI mass spectrometry. A mismatch (MM) version of this ON (14) was also synthesized using the same procedure.

Synthesis of TAMRA-623-TRI-C₆-SH (15). The 5'-thiol functionality was generated by treating the disulfide bond of the oligonucleotide (13, 40.7 nmol) with 200 μL of 100 mM of aqueous dithiothreitol (DTT) in 0.1 M TEAA buffer containing 1% triethylamine. After 30 min reaction, DTT was removed by gel filtration with a GE Healthcare illustra NAP-25 column.

After the evaporation of water, the sample was immediately used for the next conjugation reaction. A mismatch version (16) was also synthesized by the same procedure.

Synthesis of Trivalent-Bombesin Conjugated 623 Oligonucleotide (Tri-BBN-623-T, 7). Trithiol oligonucleotide (15, 67.9 nmol) was reacted with the maleimide-containing bombesin peptide (240 nmol) in a reaction buffer (final salt concentration adjusted to 400 mM KCl, 40% aqueous CH₃CN, total solution 400 μ L). The reaction mixture stood for 1 h. Purification of the oligonucleotide was carried out by reverse-phase HPLC using a ZORBAX 300 SB-C18 column (9.4 mm \times 250 mm). Finally, the product was dialyzed with Slide-A-Lyzer Dialysis Cassette (3500 MWCO, Thermo Scientific). The structure of the ON was determined by ESI mass spectroscopy.

Synthesis of Trivalent Bombesin-His6 Conjugated 623 Oligonucleotide (Tri-BBN-His6-623-T, 8). Trithiol oligonucleotide (15, 40.7 nmol) was reacted with the maleimide-containing Bombesin-His6 peptide (230 nmol) in a reaction buffer (final salt concentration adjusted to 400 mM KCl, 40% aqueous CH₃CN, total volume 600 μ L). The reaction mixture stood for 23 h. Precipitation occurred after the addition of the peptide to the oligonucleotide. After reaction, the sample was centrifuged and the supernatant buffer was carefully removed with a pipet. The precipitate was washed 4 \times with milli-Q water. Finally, the product was dissolved in formamide. Purification of the conjugate was via reverse phase HPLC as above. The structure of the conjugate was determined by ESI mass spectroscopy. The other trivalent-peptide conjugates 9, 10, 11 were also synthesized using the same procedure. The various conjugates could be solubilized in physiological buffer.

Luciferase Induction Studies. PC3/Luc705 cells were incubated in 24 well plates for 4 h in serum free medium with oligonucleotide 623 or its various conjugates usually at a concentration of 50 nM. Thereafter, serum was added to 1% and the incubation continued overnight. In an additional set of experiments, all of the initial incubations were done in the presence of 10% fetal bovine serum. At this point conjugates were removed and the incubation continued in medium plus 1% serum to 48 h at which time luciferase and cell protein were measured using a Fluostar Omega 96 well plate reader system (BMG, Cary, NC). All wells were normalized to protein concentration quantified by a BCA assay (Pierce, Rockford, IL). Control conjugates containing an oligonucleotide with 5 mismatches (623MM) were also tested.

Time Course of Oligonucleotide Mediated Induction. PC3Luc705 cells were seeded in 24 well plates and allowed to adhere overnight. Concentration of oligonucleotide stock, 623-TAMRA and Tri-BBN-His-623-TAMRA, was measured at OD260 nm prior to treatment. Cells were washed in PBS after which 400 μ L OptiMEM media was added to each well and the correct volume of oligonucleotide stock was pipetted directly into each well to achieve a 50 nM concentration. Cells were incubated at 37 $^{\circ}$ C for 24, 48, 72, or 96 h and harvested for luciferase and protein analysis as above.

Confocal Analysis of Subcellular and Nuclear Colocalization. PC3Luc705 cells were seeded in 4 well chamber slides in 10% FBS F12K media and allowed to adhere overnight. Cells were washed in PBS and OptiMEM media was added to each well after which oligonucleotide, 623-TAMRA, Tri-BBN-623-TAMRA, or Tri-BBN-His-623-Tamra was pipetted into the well and cells were incubated at 37 $^{\circ}$ C for 48 h. Cells were washed with PBS and then incubated at 37 $^{\circ}$ C for 20 min with 4 μ M Hoechst 33342 (Life Technologies) in 10% FBS F12K

media. Hoechst 33342 was washed out and 1% F12K media was added to cells. Images were captured on a Olympus FV1000 confocal microscope using a Plapon 60 \times , 1.42 NA oil immersion objective (Olympus). Multiple fields of healthy cells were sequentially imaged for TAMRA (549ex/580em) and Hoechst 33342 (405ex/450em) fluorescence. Colocalization of the two emissions was quantified using ImageJ with the JACoP plugin and is represented as Manders colocalization coefficient. In some cases, cells were transfected with baculovirus vectors that express chimeras of Green Fluorescent Protein and marker proteins for various endomembrane compartments (Life Technologies, Organelle Lights).

Uptake Studies. Cell uptake of TAMRA-labeled oligonucleotides and conjugates as a function of time in serum free medium or in the presence of 10% fetal bovine serum was measured on the Fluostar Omega plate reader system. Values were normalized to cell protein using a BCA assay.

RESULTS

The conjugates we prepared are composed of a 2'-O-methyl phosphorothioate splice switching antisense oligonucleotide (SSO623) covalently linked to peptides that contain a sequence derived from bombesin, several histidine residues, or both. An example is illustrated in Figure 1. We examined the biological

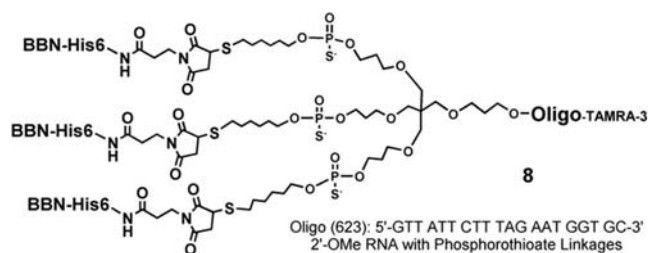


Figure 1. Bombesin–histidine–oligonucleotide conjugate. This depicts one of the multivalent conjugates produced. Three peptides containing the bombesin targeting ligand as well as six histidines are conjugated to a single 2'-O-methyl phosphorothioate splice switching oligonucleotide (oligo 623) via a trimeric linker. The conjugate is also labeled with a TAMRA fluorophore at the 3' position of the oligonucleotide.

properties of both monovalent and trivalent versions of these conjugates, as well as appropriate mismatched controls. The experimental system utilized prostate cancer cells that express the receptor for bombesin and that are stably transfected with a reporter cassette containing the luciferase coding sequence interrupted by an abnormal intron (PC3/Luc705 cells). Effective delivery of an appropriate SSO results in correction of splicing and up-regulation of luciferase expression, thus providing a convenient positive readout of oligonucleotide delivery to the nucleus.²²

The synthesis of the various conjugates is depicted in Scheme 1. The characteristics of the various conjugates, including molecular weights obtained by mass spectrometry, are listed in Table S2. Synthesis of monovalent conjugates (2–6) closely followed procedures that we have previously described,²² while the synthesis, purification, and analysis of trivalent bombesin–histidine conjugates (7–11) is described here. Analysis of the various purified conjugates is provided in Figure S1 of the Supporting Information. All of the conjugates used in this study were able to migrate in nondenaturing 20%

polyacrylamide gels, indicating that they exist as molecular species and not as highly aggregated material.

Several of the conjugates were evaluated for their ability to achieve correction of splicing and thus luciferase induction in the PC3/Luc705 cell system. In these experiments the cells were simply incubated with the various oligonucleotides in the absence of any transfection agent. As seen in Figure 2, at a

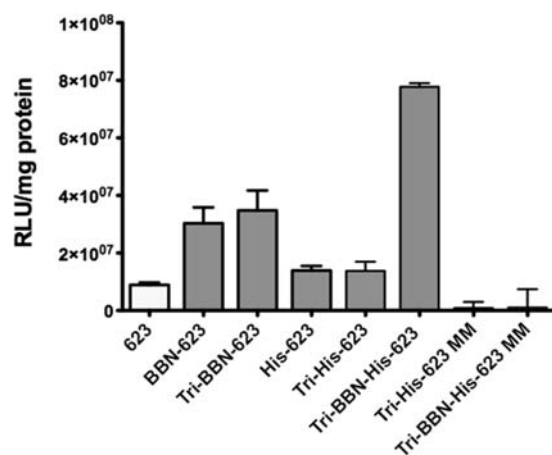


Figure 2. Biological effects of the oligonucleotide conjugates. The conjugates were tested for their ability to correct splicing and thus induce luciferase expression in the PC3/Luc705 cell system. Results are expressed as relative luminescence units (RLUs) per milligram cell protein. Means and standard errors are shown. $N = 3-5$. The concentration was 50 nM and the incubation period 48 h.

concentration of 50 nM oligonucleotide, the trimeric conjugate Tri-BBN-His-623 (8), with bombesin and six histidine residues per peptide, was substantially more effective than monovalent BBN-623 (2) or than trivalent conjugates that containing only bombesin peptide (7) or only the six histidine residues (9). Conjugates with a mismatched version of the 623 sequence (10, 11) were completely ineffective. The inclusion of histidine residues in a monovalent bombesin conjugate did not improve the effect over bombesin alone; thus, multivalency is important (Figure S2). Experiments in the presence of 10% serum showed a slight decline in effectiveness of the conjugates but the overall pattern was maintained (Figure S3). These differences in luciferase induction likely indicate differences in delivery effectiveness, since direct transfection of the various conjugates into cells via electroporation revealed only modest differences between the compounds (Figure S4) that did not parallel the differences seen in the incubation studies in intact cells.

Dose–effect and time–effect relationships for the conjugates are shown in Figure 3A,B. These studies demonstrated that the Tri-BBN-His-623 conjugate had a stronger effect than several other oligonucleotides and that the onset of the effect was more rapid. We also examined trimeric conjugates with fewer than six histidines per peptide (see Table S2), but these were significantly less effective (not shown).

We examined the uptake and subcellular localization of the TAMRA labeled conjugates using fluorescence detection and confocal microscopy. As seen in Figure S5A, the Tri-BBN-His-623 conjugate was taken up to a greater degree than Tri-BBN-623 or 623 itself. This pattern was also seen in the presence of 10% serum (Figure S5B). Confocal images in live cells showed that most of the accumulated Tri-BBN-His-623 was in cytoplasmic vesicles including substantial colocalization with

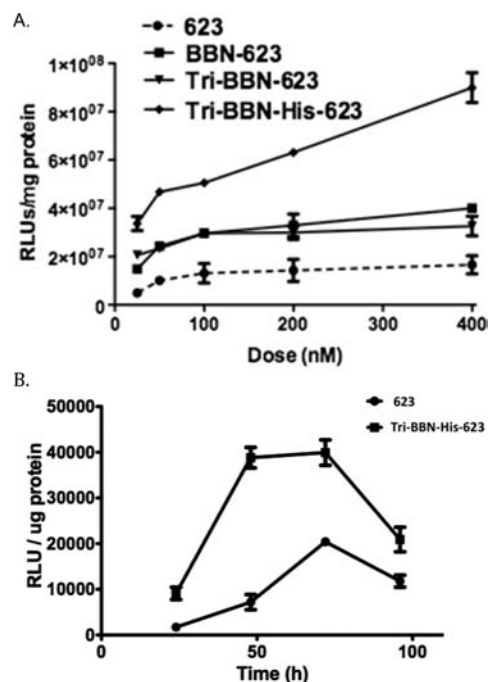


Figure 3. (A) Dose–response. Using similar conditions as in Figure 2, several of the conjugates were tested at various concentrations ranging from 25 to 400 nM. Incubation period 48 h. (B) Time–response. Using similar conditions, the ability of 623 and Tri-BBN-His-623 to induce luciferase was tested as a function of incubation time. Concentration 50 nM. Means and standard errors shown. $N = 3$.

the late endosomal marker Rab7, similar to the localization 623 itself (Figure 4A,B); this is comparable to the typical subcellular distribution of SSOs or antisense oligonucleotides.²⁸ However, colocalization studies using the nuclear marker dye Hoechst 33342 revealed a significant increase in nuclear localization for Tri-BBN-His-623 as compared to the other oligonucleotides (Figure 5A,B). Use of the Manders coefficient to evaluate colocalization, as done here, is essentially independent of the total fluorescence signal and thus gives a reliable estimate.²⁹ Since phosphorothioate oligonucleotides that enter the cytosol rapidly relocate to the nucleus, this suggests that the conjugate is escaping from endosomes and reaching the nucleus to a greater degree than the other oligonucleotides tested.

DISCUSSION

We find that inclusion of multiple histidine residues in a targeted oligonucleotide conjugate provides a significant increase in pharmacological effectiveness. Several factors may contribute to this phenomenon. First, the Tri-BBN-His-623 conjugate is taken up to a greater degree than other conjugates. However, it is unlikely that increased cell uptake accounts for all of the increased effectiveness. As we have reported previously, intracellular processing as well as cell uptake contributes to pharmacological effects.^{20,22} For example, the Tri-BBN-623 conjugate is no more effective than the monovalent BBN-623 conjugate even though the trivalent form is taken up to a greater extent. The inclusion of multiple histidine residues in Tri-BBN-His-623 was designed to provide an endosome escape effect. Our studies on nuclear localization using the Hoechst dye marker suggests that this is indeed taking place to some degree. However, the presence of histidine residues alone does not provide any substantial enhancement

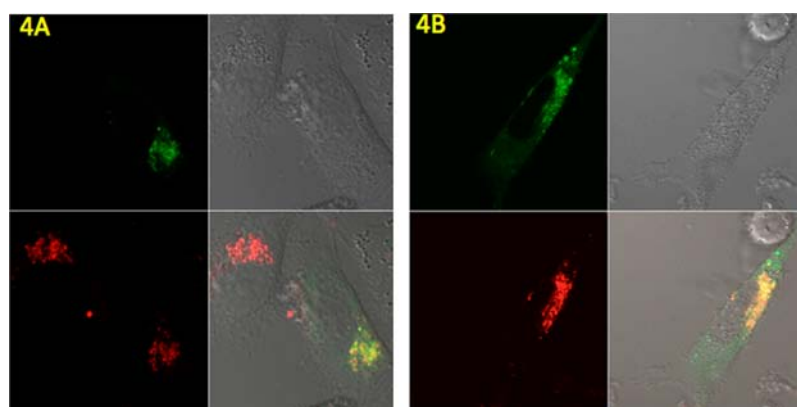


Figure 4. Subcellular distribution. Cells were transfected with a baculovirus expression vector for a Rab7-GFP chimera and subsequently incubated overnight with 200 nM of (A) 623-TAMRA or (B) Tri-BBN-His-623-TAMRA. In each panel the upper left is GFP fluorescence, upper right phase contrast, lower left TAMRA fluorescence, lower right overlap image.

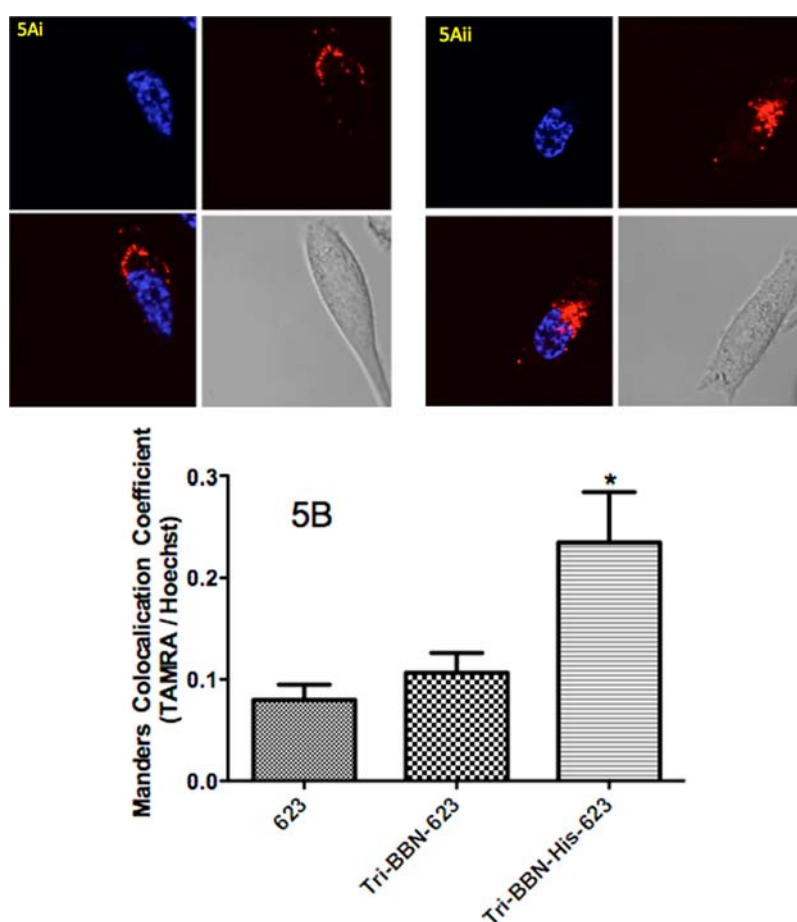


Figure 5. Nuclear localization. The subcellular distribution of conjugates in living cells was examined using confocal microscopy. (A) Cell images: (i) Tri-BBN-623-TAMRA, (ii) Tri-BBN-His-623-TAMRA. Upper left panel in each case is Hoechst 33342 fluorescence, upper right is TAMRA fluorescence, lower left is the overlap image, lower right phase contrast. (B) Quantitation of nuclear localization. The degree of overlap between the TAMRA labeled oligonucleotides and the nuclear dye Hoechst 33342 was quantitated by calculation of the Manders coefficient. Means and standard errors are shown. $N = 13-15$.

over the unconjugated SSO. Thus, the bombesin targeting function also clearly plays a role.

The increase in pharmacological effect demonstrated by the current conjugates is modest and may not be of therapeutic significance. However, this study demonstrates that it is possible to enhance the effectiveness of molecular scale oligonucleotide conjugates by rational design, addressing both

uptake and endosome escape issues simultaneously. A variety of approaches could be followed to pursue increased effectiveness. These might include use of longer histidine sequences, incorporating more than one active oligonucleotide in the conjugate, or increasing the valency of the conjugates. Thus, it seems likely that future studies will evolve novel conjugates with substantially greater effectiveness.

■ ASSOCIATED CONTENT

■ Supporting Information

Two tables, four figures. This material is available free of charge via the Internet at <http://pubs.acs.org>.

■ AUTHOR INFORMATION

Corresponding Author

*E-mail: arjay@med.unc.edu.

Present Address

Osamu Nakagawa is currently at Osaka University of Pharmaceutical Sciences 4–20–1 Nasahara, Takatsuki, Osaka 569–1094, Japan.

Notes

The authors declare no competing financial interest.

■ ACKNOWLEDGMENTS

This work was supported by NIH grant R01CA151964 to R.L.J. We thank Novatia LLC for assistance with electrospray ionization (ESI) mass spectrometry.

■ REFERENCES

- (1) Bennett, C. F., and Swayze, E. E. (2010) RNA targeting therapeutics: molecular mechanisms of antisense oligonucleotides as a therapeutic platform. *Annu. Rev. Pharmacol. Toxicol.* 50, 259–93.
- (2) Burnett, J. C., and Rossi, J. J. (2012) RNA-based therapeutics: current progress and future prospects. *Chem. Biol.* 19, 60–71.
- (3) Krutzfeldt, J., Rajewsky, N., Braich, R., Rajeev, K. G., Tuschl, T., Manoharan, M., and Stoffel, M. (2005) Silencing of microRNAs in vivo with 'antagomirs'. *Nature* 438, 685–9.
- (4) Kole, R., Krainer, A. R., and Altman, S. (2012) RNA therapeutics: beyond RNA interference and antisense oligonucleotides. *Nat. Rev. Drug Discovery* 11, 125–40.
- (5) Soldati, C., Bithell, A., Conforti, P., Cattaneo, E., and Buckley, N. J. (2011) Rescue of gene expression by modified REST decoy oligonucleotides in a cellular model of Huntington's disease. *J. Neurochem.* 116, 415–25.
- (6) Vollmer, J., and Krieg, A. M. (2009) Immunotherapeutic applications of CpG oligodeoxynucleotide TLR9 agonists. *Adv. Drug Delivery Rev.* 61, 195–204.
- (7) Chin, J. Y., and Glazer, P. M. (2009) Repair of DNA lesions associated with triplex-forming oligonucleotides. *Mol. Carcinog.* 48, 389–99.
- (8) Vaishnaw, A. K., Gollob, J., Gamba-Vitalo, C., Hutabarat, R., Sah, D., Meyers, R., de Fougères, T., and Maraganore, J. (2010) A status report on RNAi therapeutics. *Silence* 1, 14.
- (9) Watts, J. K., and Corey, D. R. (2012) Silencing disease genes in the laboratory and the clinic. *J. Pathol.* 226, 365–79.
- (10) Juliano, R., Bauman, J., Kang, H., and Ming, X. (2009) Biological barriers to therapy with antisense and siRNA oligonucleotides. *Mol. Pharm.* 6, 686–95.
- (11) Whitehead, K. A., Langer, R., and Anderson, D. G. (2009) Knocking down barriers: advances in siRNA delivery. *Nat. Rev. Drug Discovery* 8, 129–38.
- (12) Schroeder, A., Levins, C. G., Cortez, C., Langer, R., and Anderson, D. G. (2010) Lipid-based nanotherapeutics for siRNA delivery. *J. Intern. Med.* 267, 9–21.
- (13) Aliabadi, H. M., Landry, B., Sun, C., Tang, T., and Uludag, H. (2012) Supramolecular assemblies in functional siRNA delivery: where do we stand? *Biomaterials* 33, 2546–69.
- (14) Tamura, A., and Nagasaki, Y. (2010) Smart siRNA delivery systems based on polymeric nanoassemblies and nanoparticles. *Nanomedicine (London)* 5, 1089–102.
- (15) Hobel, S., and Aigner, A. (2013) Polyethylenimines for siRNA and miRNA delivery in vivo. *Wiley interdisciplinary reviews. Nano-medicine and nanobiotechnology* 5, 484–501.
- (16) Andaloussi, S. E., Lehto, T., Mager, I., Rosenthal-Aizman, K., Oprea, I. I., Simonson, O. E., Sork, H., Ezzat, K., Copolovici, D. M., Kurrikoff, K., Viola, J. R., Zaghloul, E. M., Sillard, R., Johansson, H. J., Said Hassane, F., Guterstam, P., Suhorutsenko, J., Moreno, P. M., Oskolkov, N., Halldin, J., Tedebark, U., Metspalu, A., Lebleu, B., Lehtio, J., Smith, C. I., and Langel, U. (2011) Design of a peptide-based vector, PepFect6, for efficient delivery of siRNA in cell culture and systemically in vivo. *Nucleic Acids Res.* 39, 3972–87.
- (17) Presente, A., and Dowdy, S. F. (2013) PTD/CPP peptide-mediated delivery of siRNAs. *Curr. Pharm. Des.* 19, 2943–7.
- (18) Dassie, J. P., Liu, X. Y., Thomas, G. S., Whitaker, R. M., Thiel, K. W., Stockdale, K. R., Meyerholz, D. K., McCaffrey, A. P., McNamara, J. O., 2nd, and Giangrande, P. H. (2009) Systemic administration of optimized aptamer-siRNA chimeras promotes regression of PSMA-expressing tumors. *Nat. Biotechnol.* 27, 839–49.
- (19) Kortylewski, M., Swiderski, P., Herrmann, A., Wang, L., Kowolik, C., Kujawski, M., Lee, H., Scuto, A., Liu, Y., Yang, C., Deng, J., Soifer, H. S., Raubitschek, A., Forman, S., Rossi, J. J., Pardoll, D. M., Jove, R., and Yu, H. (2009) In vivo delivery of siRNA to immune cells by conjugation to a TLR9 agonist enhances antitumor immune responses. *Nat. Biotechnol.* 27, 925–32.
- (20) Alam, M. R., Dixit, V., Kang, H., Li, Z. B., Chen, X., Trejo, J., Fisher, M., and Juliano, R. L. (2008) Intracellular delivery of an anionic antisense oligonucleotide via receptor-mediated endocytosis. *Nucleic Acids Res.* 36, 2764–76.
- (21) Alam, M. R., Ming, X., Fisher, M., Lackey, J. G., Rajeev, K. G., Manoharan, M., and Juliano, R. L. (2011) Multivalent cyclic RGD conjugates for targeted delivery of small interfering RNA. *Bioconjugate Chem.* 22, 1673–81.
- (22) Ming, X., Alam, M. R., Fisher, M., Yan, Y., Chen, X., and Juliano, R. L. (2010) Intracellular delivery of an antisense oligonucleotide via endocytosis of a G protein-coupled receptor. *Nucleic Acids Res.* 38, 6567–76.
- (23) Sethi, D., Chen, C. P., Jing, R. Y., Thakur, M. L., and Wickstrom, E. (2012) Fluorescent peptide-PNA chimeras for imaging monoamine oxidase A mRNA in neuronal cells. *Bioconjugate Chem.* 23, 158–63.
- (24) Akinc, A., Querbes, W., De, S., Qin, J., Frank-Kamenetsky, M., Jayaprakash, K. N., Jayaraman, M., Rajeev, K. G., Cantley, W. L., Dorkin, J. R., Butler, J. S., Qin, L., Racie, T., Sprague, A., Fava, E., Zeigerer, A., Hope, M. J., Zerial, M., Sah, D. W., Fitzgerald, K., Tracy, M. A., Manoharan, M., Kotliansky, V., Fougères, A., and Maier, M. A. (2010) Targeted delivery of RNAi therapeutics with endogenous and exogenous ligand-based mechanisms. *Mol. Ther.* 18, 1357–64.
- (25) Tseng, Y. C., Mozumdar, S., and Huang, L. (2009) Lipid-based systemic delivery of siRNA. *Adv. Drug Delivery Rev.* 61, 721–31.
- (26) Midoux, P., Pichon, C., Yaouanc, J. J., and Jaffres, P. A. (2009) Chemical vectors for gene delivery: a current review on polymers, peptides and lipids containing histidine or imidazole as nucleic acids carriers. *Br. J. Pharmacol.* 157, 166–78.
- (27) Prongidi-Fix, L., Sugawara, M., Bertani, P., Raya, J., Leborgne, C., Kichler, A., and Bechinger, B. (2007) Self-promoted cellular uptake of peptide/DNA transfection complexes. *Biochemistry* 46, 11253–62.
- (28) Juliano, R. L., Ming, X., and Nakagawa, O. (2011) Cellular uptake and intracellular trafficking of antisense and siRNA oligonucleotides. *Bioconjugate Chem.* 23, 147–57.
- (29) Dunn, K. W., Kamocka, M. M., and McDonald, J. H. (2011) A practical guide to evaluating colocalization in confocal microscopy. *Am. J. Physiol. Cell Physiol.* 300, C723–742.